Light Commercial Vehicle ADAS-Oriented Modelling: An Optimization-Based Conversion Tool from Multibody to Real-Time Vehicle Dynamics Model

Light commercial vehicle ADAS-oriented modelling: an optimization-based conversion tool from multibody to real-time vehicle dynamics model

Author, co-author (Do NOT enter this information. It will be pulled from participant tab in MyTechZone)

Affiliation (Do NOT enter this information. It will be pulled from participant tab in MyTechZone)

Abstract

In the last few years, the number of Advanced Driver Assistance Systems (ADAS) on road vehicles has been increased with the aim of dramatically reducing road accidents. Therefore, the OEMs need to integrate and test these systems, to comply with the safety regulations. To lower the development cost, instead of experimental testing, many virtual simulation scenarios need to be tested for ADAS validation. The classic multibody vehicle approach, normally used to design and optimize vehicle dynamics performance, is not always suitable to cope with these new tasks; therefore, real-time lumped-parameter vehicle models implementation becomes more and more necessary. This paper aims at providing a methodology to convert experimentally validated light commercial vehicles (LCV) multibody models (MBM) into real-time lumped-parameter models (RTM). The proposed methodology involves the definition of the vehicle subsystems and the level of complexity required to achieve a good match between the simulation results obtained from the two models. Thus, an automatic vehicle model converter will be presented together with the assessment of its accuracy. An optimization phase is included into the conversion tool, to fine-tune uncertain vehicle parameters and to compensate for inherent modelling differences. The objective function of the optimization is based on typical performance indices used for vehicle longitudinal and lateral dynamics assessment. Finally, the simulation results from the original and converted models are compared during steady-state and transient tests, to prove the conversion fidelity.

Introduction

Following the new regulations in terms of active and passive safety, the new and always more demanding requests from the markets, the supplementary performances required and the increasing of technology level, complexity in vehicles is a key point to be considered. Therefore, vehicle design, verification and validation are crucial milestones regarding each phase and the interaction among themselves. To fulfill all these requirements, a complete methodology and workflow have been developed. It consists of a creation of a virtual environment in which it is possible to verify and validate different vehicle configurations both in terms of dynamics, stability, performances [1], and its interaction with its surroundings. Thanks to the integration of sensors and control logics, it is possible to develop process optimization, enlarge test scenarios, and reduce the number of physical tests. In addition, early detection of integration issues and more realistic correlation with proving ground test results are feasible. The use of multibody modelling for vehicle dynamics studies and comfort assessment and validation has been widely used, see e.g., [2-3], for heavy commercial vehicles. The multibody experimental-numerical correlation is also applied to other vehicles categories, as done by [4], to enhance the performance for motorsport applications. Multibody validation is applied to LCVs, which are the subject of this work, in [5] where handling studies on the safety limits are presented. The highly detailed multibody models need to be simplified to cope with massive ADAS system testing. This involves the necessity to drastically reduce the computational time of simulations. The lumped parameter approach offers the advantage to perform real-time simulation and hardware-in-the-loop testing, in which ADAS can be investigated in realistic driving scenarios. On the other hand, any modification of the vehicle's suspension and steering systems implies a new conversion process from the multibody model; furthermore, second-order effects on vehicle dynamics, such as component flexibility, are not considered by these simplified lumped-parameter models. Different approaches are available in the literature. This problem investigated by [6], where a simplified 16 DoF LCV model is proposed, combining the multibody formulation with a real-time solver implementation. Other authors [7] propose a method to enhance the simulation performance using a real-time multibody vehicle model, starting from an ADAMS/Car reference model, exploiting an approximate function approach for the suspension subsystem. As well known, suspension represents a critical part to be treated, so the level of detail to be considered is a crucial aspect for this work. The model order reduction is the main theme presented in [8], where a robust methodology to obtain fast single track vehicle models is presented, by using a map identification approach from the reference vehicle. Thus, a methodology to properly convert the main subsystem of the multibody model into a real-time one is largely investigated. To achieve this challenging task that OEMs must face, the development of an automatic conversion tool is very helpful. Conversion tools from multibody to different real-time vehicle models (CarSim, Carmaker, VI-CarRealTime) have been implemented in dedicated commercial software called AutoConvA2C© and ADAMS2CM [9-10] or directly integrated into the real-time software [11]. In this context we developed a conversion tool, in MATLAB environment, for IPG CarMaker [12], that stands out, with respect the commercially available tools, for the presence of a novel optimization phase; this can improve model fitting between the two environments, by tuning properly the uncertain parameters. The use of different optimization tools for the estimation or tuning of some vehicle characteristics is present in previous works. The genetic algorithm (GA) is chosen by [13] to identify the tire parameters of Pacejka models, by [14] to optimize the vertical stiffness and damping characteristic of simplified suspension model with experimental data, and by [15] to find the optimal design parameter of a transmission gearbox. Finding a good estimation of the uncertain parameters, as geometrical and material properties on mode shape is a key role presented by [16], which use the fmincon algorithm for a FEM model of a spoke wheel. Other works

involve the usage of DOE analysis for suspension optimization as done by [17].

The main features of the conversion tool presented here are:

- automatic real-time vehicle model generation in IPG.CarMaker;
- reliable conversion method guaranteed by the optimization loop, for different vehicles size/weight.
- fast execution (one working day with a standard PC to obtain the optimized converted vehicle)
- easy to use graphical user interface
- two user modes (standard and expert) to set standard /advanced parameters for the optimization phase.

This paper aims at presenting the methodology and the results obtained with the developed conversion tool. The first part regards the presentation of the methodology and the definition of the uncertain and the certain parameters. Then, the multibody vehicle model, used as reference, is illustrated. The main assumptions on the level of complexity adopted in the real-time software for the different subsystems (suspension, body, steering, etc.) are exposed. Furthermore, the optimization algorithm is presented, by describing the selected tunable parameters and the objective function. Then, an LCV case study is analyzed and a comparison between the reference multibody vehicle model and the converted real-time one, focused on the conversion fidelity, is shown. Finally, conclusions on the presented method are drawn.

Methodology

In this section, the methodology adopted for the development of the conversion tool is presented. The transition from multibody into a lumped-parameter modelling approach involves a model order reduction that requires the following steps to obtain a good convergence:

- define the level of complexity for each vehicle subsystem;
- distinguish the parameters directly convertible through lookup tables and/or gains, from the ones that require a dedicated tuning.

The first aspect is related to the structural differences between the subsystems modelling employed by the two software. For instance, the real-time software offers different possibilities for suspension kinematics modelling, e.g., using 1D or 2D linear or nonlinear maps. The second aspect instead, is related to the distinction between the uncertain and the certain parameters. Certain parameters involve the direct conversion from the multibody software to the real time one, without any model order reduction. This can be done when the same modelling approach is adopted by the two software for a specific subsystem, like for the tire model. Conversely, the uncertain parameters are chosen when a different level of approximation is adopted by the two software. In fact, we pass from a physical model with a high number or degree of freedom to a lumped parameter model, composed by 14 degrees of freedom. Moreover, a parameter is chosen tunable if it significantly modifies the dynamic behavior of the vehicle and therefore it can facilitate the convergence of the optimization process. The certain parameters belong to:

- tire properties: the two models share the same Pacejcka MF-tire model;
- suspension elasto-kinematics: the real-time software provides different ways to compute the wheel spatial motion, depending on the level of complexity of the converted suspension. It spans from a linear description to a more detailed nonlinear mono or multidimensional map as a function of the wheels travel, steering rack travel (kinematics), forces and moments (compliance) applied to each wheel;
- brake system: pedal to brake torque actuation gain;
- powertrain: gear ratio, final drive ratio, engine and flywheel mass moments of inertia.

The tunable parameters are:

- suspension parameters, like stiffnesses and damping characteristic, due to their strong influence on vehicle handling behavior;
- sprung/unsprung mass and moments of inertia: the large reduction of degrees of freedom forces to compute equivalent lumped mass and moment of inertia. A variable percentage of the suspension linkages can be attributable to sprung or unsprung mass; more details will be given in the dedicated section;
- center of gravity (CoG) height;
- engine torque map amplification gain.

Therefore, these parameters will be used in the optimization loop, to compensate for the modelling discrepancies and to improve the performance fitting.

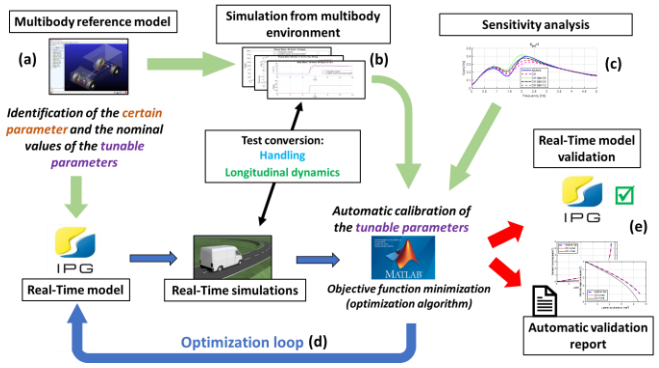

Figure 1 – Workflow of the conversion tool

The conversion workflow is shown in Figure 1. The conversion process is composed by two steps: a direct conversion of the multibody model and an optimization phase, the second being optional. The multibody model constitutes the source of information of the conversion process in terms of vehicles data (a) necessary for the conversion phase and the results of the simulations (b) used as reference by both the two steps mentioned above. The vehicle information is collected either directly from the property files or by exploiting some multibody software tools (for instance to get equivalent inertial properties). Before starting the optimization loop a sensitivity analysis (c) on tunable parameters is carried out as preparatory phase for the vehicle optimization. In this way the range of each uncertain parameter can be identified. When the optimization loop starts (d), the patternsearch algorithm [20] minimizes a properly designed objective function, based on typical performance indices, by tuning the uncertain parameters. Finally, the simulation comparison of the two models are shown in a report containing the validation results and the optimization performance level (e). The conversion, optimization and report generation phases are completely performed in MATLAB environment.

Multibody model description

The methodology has been applied to light commercial vehicles, with a weight ranging from 3,5 tons to 7 tons. The vehicles under investigation feature front-engine rear-wheel-drive layouts. The LCV multibody model is characterized by the following subsystem:

- front suspension,
- rear suspension,
- steering system,
- powertrain,
- wheels.

A brief description of the main subsystems is given in the following sections.

Front suspension

The LCVs under investigation adopt two types of front suspension: QuadLeaf and QuadTor. The first one is used for small size LCV (i.e., the 3,5 tons one). It is characterized by a double wishbone design with a transverse mono-leaf spring. This leaf spring connects elastically the two wheels, thus fulfilling two functions: it acts like a spring in the parallel wheel travel and like an antiroll bar in the opposite wheel travel. For heavier LCVs sizes (e.g., from 4,0 tons to 7 tons) the so-called QuadTor solution is preferred. The double wishbone suspension is still present, but the leaf-spring is substituted by a couple of longitudinal torsion bars and an antiroll bar. Figure 2 shows the MBM adopted for the front suspension.

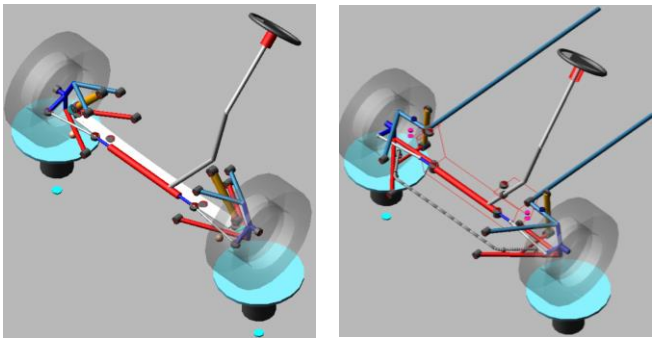

Figure 2 – Front suspension adopted for LCV: QuadLeaf on the left, QuadTor on the right.

Rear suspension

The rear suspension is a solid axle suspension, housing the differential and the half-shafts. Longitudinal leaf springs are the only components used to constrain, by means of their eyes and shackles, the axle to the vehicle body, therefore all the forces and moments exchanged between the axle and the vehicle body pass through them. For the smallest size LCVs (3.5 tons), single-leaf spring is adopted, while for heavier LCVs multi-layered semielliptical leaf springs are used; in addition, the tires from single become dual. An antiroll bar is also installed to increase the suspension roll stiffness.

The MBM includes the driveline inside the solid axle, i.e., the differential and the driveshafts; the latter are mounted inside a hollow beam flexible body to model the deformation under load of the axle. Figure 3 shows the adopted configuration for the rear suspension.

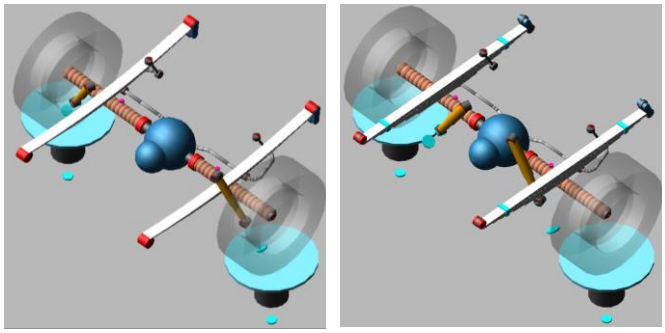

Figure 3 – Rear suspension adopted for LCV: single leaf spring on the left, multi-layer leaf springs on the right.

Even though the front and rear suspension vary among the different vehicle versions (having different gross vehicle weights), the presented conversion method remains the same. In fact, the structure of the suspension model adopted in the real-time software is the same, regardless of the actual design, as will be detailed later in the article.

Steering system

The MBM features a passive rigid steering system (no torsion bar and power steering) having three shafts connected through two constant velocity joints. The motion from the lower shaft is transmitted through the rack and pinion mechanism towards the steering wheels, thus achieving a quasi-Ackermann steering condition. In Figure 4 the main parts of the MBM steering subsystem are highlighted.

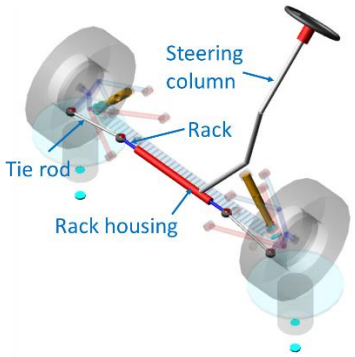

Figure 4 – Steering system used in the multibody model.

Real-Time model description

The conversion tool generates a 14 degrees of freedom (DoF) model characterized by:

- 6 DoF for the vehicle chassis, namely the sprung mass
- 8 DoF (= 2DoF x 4 wheels) for the unsprung masses. The 2DoF for each wheel are the wheel vertical travel and the wheel spin.

The MBM subsystems are converted by exporting parameters or lookup tables from the components property files and suspension analysis results.

Suspension and steering

The RTM suspension subsystem can be defined, through lookup tables or gains, depending on the data available. These can be obtained from virtual or experimental kinematics and compliance (k&c) testing and from the components data property files. In this work, the map-based approach is used, allowing to describe every type of suspension, regardless of the specific suspension design. The selection of the level of detail for the suspension motion description is a key aspect in this method. This section is focused on the conversion of each suspension part, i.e., k&c, suspension stiffnesses, dampers and buffers.

Kinematics and compliance

The kinematics and compliance or elasto-kinematics characteristic of a suspension is the description of the spatial motion of each wheel (relative to the chassis) caused by quasi-static application of realistic displacements and loads to the wheel itself. The quasi-static k&c tests are commonly used for suspension characterization, but some authors [10] extend the application on dynamic test, to understand the effect on the body stiffnesses. In the kinematic part the wheel vertical bump and the steering rack displacement are varied, while forces and moments are applied in the compliance part. With the following equation the wheel position and orientation are computed by effects superimposition of kinematics (Kin) and compliance (Com) maps:

$$\begin{bmatrix} t \\ r \end{bmatrix} = \sum_i Kin(x_r, z_p, z_o) + \sum_i Com(F_x, F_y, M_x, M_y, M_z) \tag{1}$$

where vector t contains the three components of the wheel center translation t_x, t_y, t_z , while vector r includes the three components of its rotation r_x, r_y, r_z. Translations and rotations are evaluated with respect to the vehicle body. The maps are obtained from the MBM by executing a dedicated routine that sets up and runs a series of suspension analysis, i.e., parallel/opposite wheel travel and load case tests (static application of forces and moments to the wheel).

Kinematics

In this work the suspension kinematics is modelled by using 2D nonlinear lookup tables that are generated by parallel and opposite compression test in the multibody environment, for both front and rear suspensions. The maps require as input different generalized coordinates, depending on whether the suspension is an independent wheel suspension or a dependent wheel suspension:

- front suspension: parallel wheel travel z_p and rack position x_r, Figure 5 (a);
- rear suspension: parallel wheel travel z_p and opposite wheel travel z_o, Figure 5 (b).

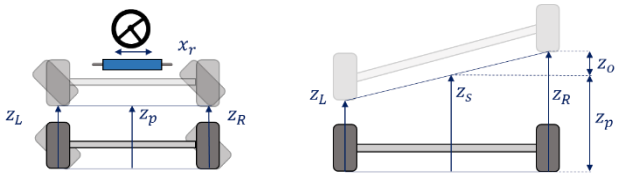

Figure 5 – Procedure to obtain kinematics quantities for the front suspension (a) and rear suspension (b)

The parallel and opposite travels are defined as:

$$z_p = z_s = \frac{z_L + z_R}{2}; \qquad z_o = \frac{z_L - z_R}{2} \tag{2}$$

where z_L and z_R are respectively the left and right wheel travel and z_s is the suspension travel (equal to the parallel contribution). Thus, the front independent wheel suspension is characterized by analyzing all the possible combinations of the parallel wheel travel and steering, while the rear dependent wheel suspension is characterized by all the combinations of parallel and opposite wheel travel. The output quantities are listed below:

- three components of wheel center translation, denoted as t_x, t_y, t_z;
- three components of wheel rotation, that are toe angle r_z, caster angle r_y and the camber angle r_x;
- length variations of the force elements: spring, damper, stabilizer, buffer.

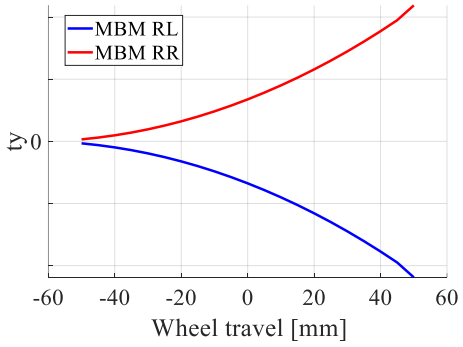

Figure 6 – Example of a rear suspension kinematics map obtained from the multibody model. Red curve: rear right. Blue curve: rear left.

The latter are used for the computation of forces by interpolating the characteristics of the components.

Figure 6 shows the results from the virtual k&c test of the parallel wheel travel for the front suspension on a wheel travel range of [-50;50] mm. Since the maps are nonlinear, a simpler modelling approach such as the one based on constant kinematic gradients would have led to unacceptable discrepancies between the two models.

Compliance

The effect of compliance on the wheel generalized displacement is described by 1D maps for both front and rear suspension. The input quantities can be represented by the longitudinal F_x or lateral forces F_y applied on wheel center, or by the moments M_x, M_y, M_z. These are applied on a single wheel, and two set of maps are obtained from each wheel:

- displacements and rotations vs force applied on the current wheel;
- displacements and rotation vs force applied on the opposite wheel.

The compliance lookup table can be obtained from suspension virtual bench in the multibody environment, in which the force is applied on the contact patch. On the other hand, the RTM uses a system of forces applied to the wheel center. Therefore, the maps related to M_x and M_y are nulled to avoid considering the same effect twice. The output quantities are the same as the ones described in the kinematics section.

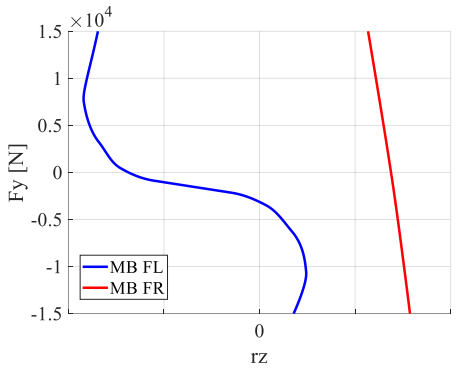

Figure 7 – Example of a front suspension compliance map obtained from the multibody model. Red curve: front right. Blue curve: front left.

Figure 7 shows the trend of the toe angles r_z subjected to a lateral force F_y applied to the left wheel (FL) of the front suspension. The curves are nonlinear, and the right wheel (FR) motion is influenced by the application of the force to the opposite wheel (FL).

Suspension vertical and roll stiffness

This section presents the procedure to characterize and model the suspension stiffnesses. Commercial real-time software for passenger cars usually distinguishes between the primary springs (one for each corner) and the antiroll bar (one for each suspension). However, since the suspension design of the analyzed LCV features a single component, i.e., a transversal leaf spring to accomplish both the tasks, a different approach must be followed. Thus, in this paper, we decide to characterize the entire suspension vertical stiffness at the wheel centers and to implement in the RTM a 1D map generated from a parallel wheel travel test executed in the multibody software; in this way, it is not necessary to import the component map, since an equivalent nonlinear characteristic, that includes all the stiffness contributions, is obtained. Figure 8 (a) shows the suspension vertical flexibility from a parallel (red line) and an opposite (blue line) wheel travel test.

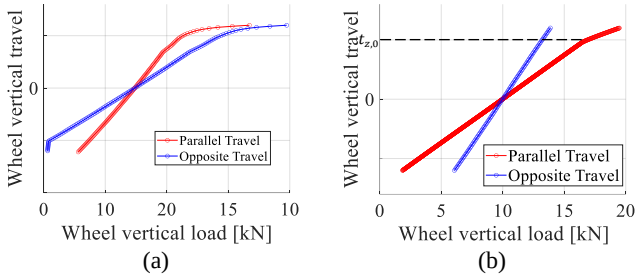

Figure 8 – Front (a) and rear (b) suspension wheel travel obtained from the multibody model. Red curve: parallel travel. Blue curve: opposite travel.

This characteristic is used to compute the value of the antiroll bar stiffness, by subtracting the contribution of the parallel stiffness from the opposite one. Both stiffnesses are applied at the wheel center. Furthermore, as the suspension test is obtained using the vertical forces applied at the contact patch, to compute them correctly, it is necessary to remove the contribution determined by the unsprung masses. The method applied to the rear suspension differs slightly for the rear suspension. The change is due to the stiffnesses characteristic of a solid axle, as can be seen in Figure 8 (b). The antiparallel stiffness (blue line) is lower than the parallel one (red line). This trend is typical, for this suspension design. Since a negative antiroll bar stiffness could not be implemented in the commercial software, we introduced an equivalent internal force. This is proportional to the opposite wheel travel through a negative gain, and acts between the sprung and unsprung mass, thus generating a reduction of roll stiffness.

Buffer and damper

The conversion of the suspension buffer and damper is performed by using the component property file stored in the multibody model. The real time software allows to import 1D nonlinear lookup table for both components. Commercial software distinguishes between compression and extension map, to characterize the bumpstop or the reboundstop depending on the direction of the wheel travel. In Figure 9, a scheme representing the damper and buffer configuration in the real time software is shown.

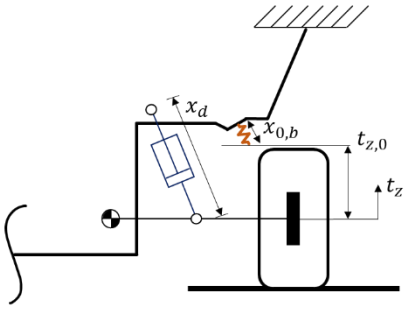

Figure 9 – Quarter car representing the equivalent swing arm used by the commercial software to compute the vertical forces contribution coming from the damper and buffer module.

Starting from the buffer length computed from the kinematic maps, the buffer forces developed at the wheel center are:

$$F_{z,bump} = \begin{cases} 0, & t_z < t_{z,0} \\ F_{bump}(x_b - x_{0,b}) \cdot \dfrac{dx_b}{dt_z}, & t_z \geq t_{z,0} \end{cases}$$

$$F_{z,rebound} = \begin{cases} 0, & t_z > t_{z,0} \\ F_{reb}(x_{0,b} - x_b) \cdot \dfrac{dx_b}{dt_z}, & t_z \leq t_{z,0} \end{cases}$$

(3)

where F_{bump} and F_{reb} are the 1D maps converted from the MBM, $t_{0,z}$ and $x_{0,b}$ are the bumpstop/reboundstop clearances, the first is measured from wheel center, the second is measured from its installation point. dx_b is the variation of the damper length and dt_z is the wheel center position variation. Similarly damping forces are computed with the following equation:

$$F_{z,damp} = F_{damp}(\dot{x}_d) \cdot \frac{dx_d}{dt_z}$$

(4)

Where F_{damp} is the 1D map converted from the MBM, $\dot{x}_d$ is the damper velocity computed as the time derivative of the damper length, extracted from the kinematic maps. dt_z is the differential of the wheel center position, while dx_d is the differential of the damper length.

Steering System

Commercial real time software offers the possibility to choose among different steering models: these span from a simple rigid steering system (Figure 10) to a more detailed one. For instance, the Pfeffer's model belongs to the last category; it includes the definition of the inertial, elastic, dissipative properties of the steering components, through a three DoFs lumped parameters model [18]. Moreover, EPS and HPS power assistance maps can be easily integrated. However, in this paper, the first model is selected, therefore, the only parameter to be converted in the real time software is the pinion to rack transmission ratio $\tau_{pin/rack}$. The remaining part of the steering mechanism, from rack to wheel, is included in the kinematics map (as explained in the suspension kinematics section).

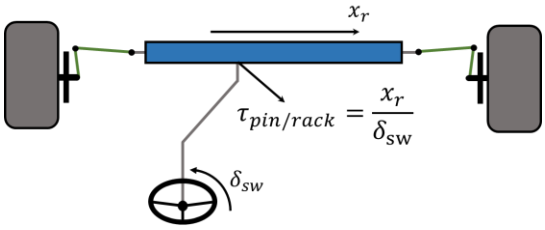

Figure 10 – Rigid steering system adopted in the conversion tool

Sprung and unsprung masses

Real-time vehicle models usually split the vehicle mass into sprung and unsprung mass, the latter having a rotating part and a non-rotating one. Since the definition of sprung and unsprung mass is not unique, but is associated with a certain amount of uncertainty, a split factor is introduced to manage this aspect. This factor may eventually be tuned during the optimization process. Using internal tools, commonly available in commercial multibody software, masses and moments of inertia can be aggregated to achieve the desired equivalent parameters for populating the real-time model. The differences between the dependent and independent suspension in managing the rotating part of the driveline are shown in the following sections.

Front suspension

The unsprung masses of the front suspension are computed with the following equation, dividing the rotating parts $m_{um,rot}$ from the non-rotating ones $m_{um,nrot}$, for each i^{th} vehicle corner:

$$m_{um,rot,i} = \sum_j m_{um,j} = m_{wheel} + m_{diskBrake} + m_{spindle}$$

$$m_{um,nrot,i} = m_{upright} + K_{umF,SuspLinks} \cdot \sum m_{um,SuspLinks}$$

(5)

where $m_{um,j}$ represents the masses of the wheel or the brake disk or the spindle and $m_{um,SuspLinks}$ is the mass of a single suspension linkage, Figure 11(a). While the rotating masses are considered 100% unsprung, because this is a driven axle, the nonrotating ones are composed by a fixed part $m_{upright}$ (suspension upright) and by a percentage of the suspension linkages, where $K_{umF,SuspLinks}$ is the split factor. Figure 11(b) shows the split between the sprung and unsprung masses.

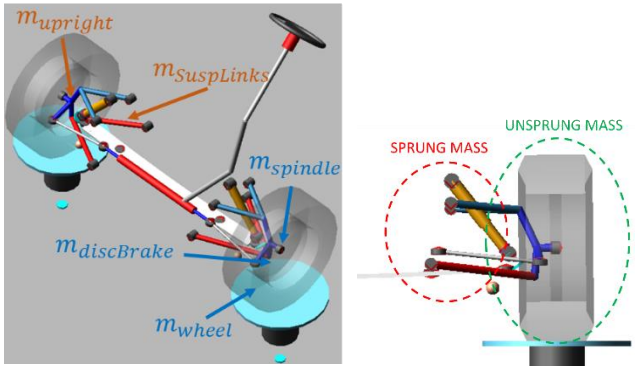

(a) (b)

Figure 11 - QuadLeaf suspension, example of aggregation of masses (a). Blue arrow for the rotating mass, orange arrow for the nonrotating one. (b) shows the uncertainty of suspension link to be split in sprung and unsprung.

Rear suspension

The rear suspension is a rear drive solid-axle suspension. This solution integrates part of the driveline into the rigid axle. Therefore, we propose to split the rotating parts into unsprung and sprung mass through another split factor $K_{um,DriveLine}$. Figure 12 shows this qualitative division: engine, transmission and a portion of the propeller shaft are included in the rotating sprung mass; the remaining part of the propeller shaft and the driveline inside the solid axle constitute the rotating unsprung mass ($m_{um,driveline}$) . Thus, for a solid axle suspension these equations hold:

$$m_{um,rot} = \sum m_{um,j} + K_{um,DriveLine} \cdot \sum m_{um,driveline}$$

$$m_{um,nrot} = \sum_{j} m_{um,fixed,j} + K_{umR,SuspLinks} \cdot \sum m_{um,SuspLinks}$$

(6)

where the fixed mass ($m_{um,fixed,j}$) for the two-rear quarter of the vehicle includes half of the hollow beam and half of the differential housing. The longitudinal leaf spring instead is attributed to the uncertain masses. The split factor is $K_{umR,SuspLinks}$.

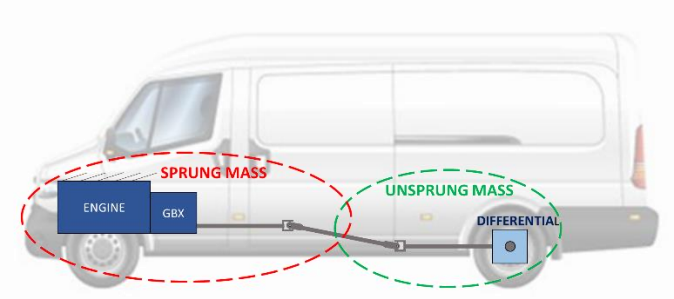

Figure 12 – LCV with front longitudinal engine and rear wheel drive.

Finally, the sprung masses are computed with this equation:

$$m_{sprung} = \sum_{j} m_{sprung,j} + \left(1 - K_{umF,SuspLinks}\right) \cdot \sum m_{umF,SuspLinks} + \left(1 - K_{umR,SuspLinks}\right) \cdot \sum m_{umR,SuspLinks} + \left(1 - K_{um,Driveline}\right) \cdot \sum m_{um,driveline}$$

(7)

where $m_{sprung,j}$ contains all the bodies considered as sprung masses, such as the engine (the powertrain mounting system is assumed rigid), the steering column and rack and the central part of the transverse leaf spring.

Optimization process

The conversion tool presented in this paper involves an optimization phase aimed at obtaining a set of uncertain parameters capable of guaranteeing the best fitting between the two models. This feature distinguishes our method from those find in the literature and in commercial software. The algorithm and the objective function formulation of the optimization problem are described in this section. The MBM simulation results of lateral and longitudinal dynamic test are used as the benchmark for the comparison between the two models. The optimization problem is formulated as:

$$X_{opt} = \arg\min f(x) : x \in [-l_b, u_b] \subseteq \mathbb{R}^n$$

(8)

Where $f(x)$ represents the objective function accounting for the deviation of the two model results, x are the tunable parameters and l_b and u_b are the vectors of the lower and upper bounds. The optimization problem is set as unconstrained and bounded.

The fitness function is computed as the average of the weighted sum of the N corrected errors $e'_{j,k}$ of the M maneuvers:

$$f(x) = \frac{1}{N}\sum_{j=1}^{N}\left(\frac{1}{M}\sum_{k=1}^{M} w_{j,k} \cdot e'_{j,k}\right)$$

(9)

The corrected error is defined as:

$$\begin{cases} e'_{j,k} = e_{j,k} + PF \cdot \left(e_{j,k} - TP\right) & \text{if} \quad e_{jk} > TP \\ e'_{j,k} = e_{j,k} & \text{otherwise} \end{cases}$$

(10)

where $e_{j,k}$ represents the RMSE associated to a specific performance index, computed by comparing the results from the converted and the reference vehicle, while $w_{j,k}$ represent the corresponding weight. To force the convergence of the algorithm in a predefined range of fitting errors between the two models, a percentage tolerance TP is introduced. A penalty factor PF is used to increases the error of a maneuver when the set of parameters chosen leads to exceeding TP. The estimation error $e_{j,k}$ is computed as the RMSE of the terms listed in the Table 1 and Table 2. These quantities are chosen for the handling and longitudinal dynamics assessment.

Table 1 – Lateral dynamics indices computed from typical steady-state and transient test, evaluated as RMSE.

Ramp steer (Maps)	Sine sweep (FRFs)	Step steer (iso 7401)
• δ_{sw} *vs* a_y • β *vs* a_y • ϑ *vs* a_y • $\Delta F_{z,tot}$ *vs* a_y	• $\left\lvert\frac{\vartheta}{\delta_{sw}}(\omega)\right\rvert$ • $\left\lvert\frac{a_y}{\delta_{sw}}(\omega)\right\rvert$ • $\left\lvert\frac{\dot{\psi}}{\delta_{sw}}(\omega)\right\rvert$	• Overshoot • Peak time • Response time • Steady State gain

Where δ_{sw} is the steering wheel angle, β is the sideslip angle, ϑ is the vehicle roll angle, $\Delta F_{z,tot}$ represents the total lateral load transfer a_y is the lateral acceleration, $\dot{\psi}$ is the yaw rate and ω represent the frequency.

Table 2 – Longitudinal dynamics indices, evaluated as RMSE.

Acceleration test	Braking test
• Velocity • Pitch angle • Front, rear vertical load	• Longitudinal deceleration • Pitch angle • Front, rear vertical load

The RTM parameters set x to be optimized is selected from the vehicle inertial and geometrical characteristics, suspension elastic and dissipative properties and engine torque characteristic:

- Chassis parameters: Sprung mass, inertia moments: I_{xx}, I_{zz}, I_{xz} , Sprung mass CoG height, front axle distance to CoG.
- Suspension parameters: front/rear amplification factor of secondary spring, front/rear antiroll bar stiffness, front/rear damper amplification factor.
- Powertrain: engine map amplification factor.

The imposed upper and lower bound are [-20%, 20%] of the nominal x values.

Results

The results of the conversion and optimization process are shown in this section. The case study proposed regards the conversion of a 7-ton laden LCV multibody model. For handling assessment, steady-state and transient maneuvers are selected, while an acceleration test for the longitudinal dynamics is presented. Considering an expert user, the estimated time to obtain a converted and optimized real-time model is of, approximately 3h for the conversion phase and approximately 8h for the optimization phase. For a PC with 16 GB of RAM, 2.3 Ghz – 8 core CPU. These values are quite obviously affected by the user ability and optimization options.

Optimization process analysis

This section aims to provide the analysis of the optimal solution obtained by the methodology described in the previous section. Figure 13 shows the percentage change of the tunable parameters optimized with respect to their nominal values.

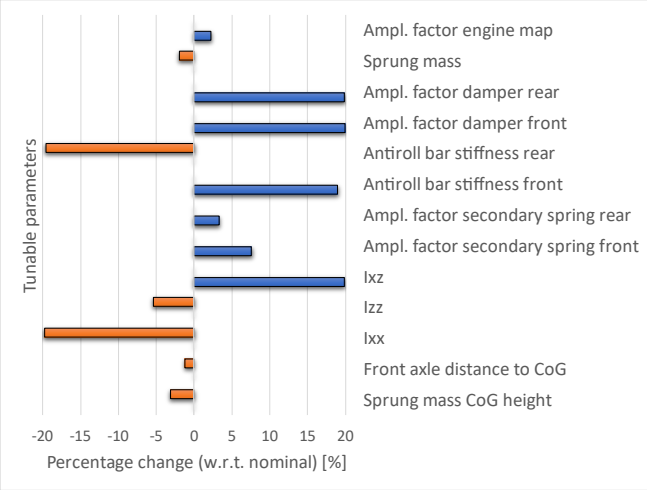

Figure 13 – Final values of the designed parameters obtained from the optimization process.

The histogram shows that the optimization pushes the values of several tunable parameters to the borders but at the same time it avoids increasing them further up to unrealistic values. The modification of the tunable parameters affects the vehicle dynamics performance, as will be illustrated in the following sections where the procedure is validated during steady-state and transient maneuvers.

Ramp steer test

This section summarizes the main results of the ramp steer maneuver. This test is performed at 80 km/h while the steering wheel angle increases with a constant slope of 5 deg/s. The methodology efficacy is evaluated through the elaboration of RMSE for the steering wheel angle, the sideslip angle, the roll angle and the total lateral load transfer. as can be also seen in the Figure 14. The process shows a good accuracy level of the first conversion and a further improvement of the optimization phase. The two models fit well in the steady-state response.

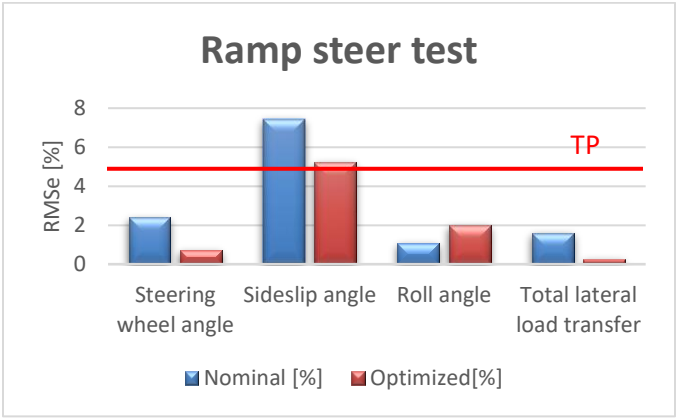

Figure 14 – RMSE of the steady-state indices. Red line refers to the TP level.

Figure 15 shows the results of the steady state characteristics. The main considerations are:

- the increase of the front stabilizer stiffness, the decrease of the rear one and the front axle distance to CoG reduction, increase the understeering behavior w.r.t the nominal configuration;
- the sideslip angle RMSE obtained with the optimized model is improved w.r.t. the nominal configuration, although it slightly exceeds the TP;
- the CoG height reduction, with the optimization process, improves the vehicle total lateral load transfer RMSE. Meanwhile, the roll angle RMSE has slightly worsened w.r.t. the nominal configuration, always remaining within the TP;

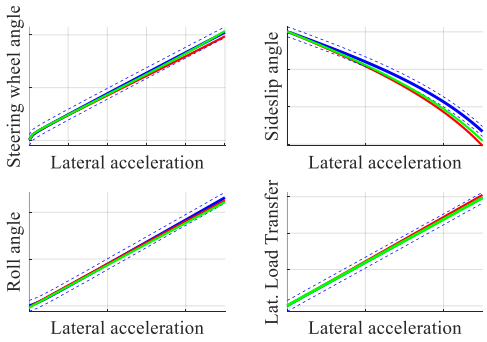

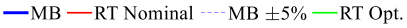

Figure 15 – Ramp steer test results

Step steer test

Figure 16 reports the results of the LCV transient response, obtained in agreement with the ISO 7401 test procedure [21]: the vehicle is tested at 100 km/h with a steering angle value of 10 deg with a very fast input velocity ~ 500 deg/s. The steering wheel angle is set to obtain 0.4g of lateral acceleration. For both lateral acceleration and yaw rate, the optimization process can tune the parameter to obtain a good converge between the two models. The initial converted vehicle shows out of range response, while after the optimization process, the results show an improvement, since the RMS error descends approximately at 2%.

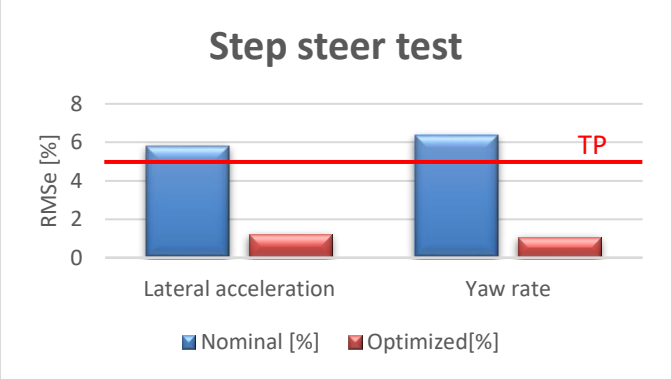

Figure 16 – RMSE of the transient tes.t Red line refers to the TP level.

Figure 17 shows the simulation results of the step steer test. The vehicle response is overdamped, as no oscillation occurs. The set of chosen parameters improve the steady-state part of the transient response, as both the lateral acceleration and the yaw rate of the RTM well fits with the reference MBM.

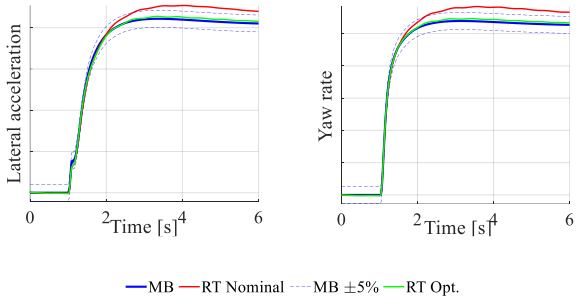

Figure 17 – Step steer test results

Acceleration Test

Finally, an acceleration test is proposed. In this maneuver the vehicle starts from 25 km/h, and it is accelerated as fast as possible reaching the maximum speed. There is a good correlation between the models and the optimization permits to obtain an RMS error below 5%, as reported in Figure 18. The maximum vehicle velocity is matched by tuning the engine map gain, as can be seen in the Figure 19.

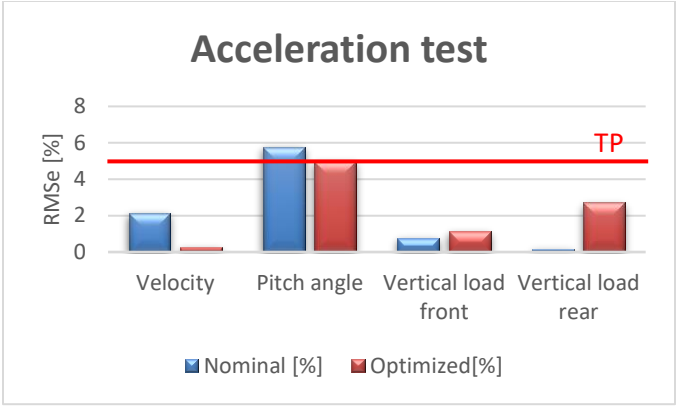

Figure 18 – RMSE of acceleration test. Red line refers to the TP level.

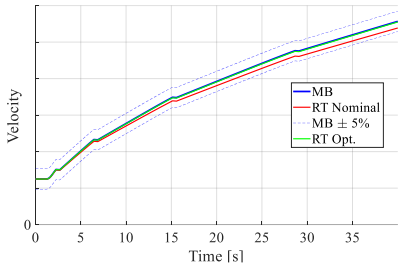

Figure 19 - Vehicle velocity in the acceleration test.

The slight increase of the secondary spring gradient in the optimized configuration increments the vehicle total roll stiffness, improving the pitch angle RMSE.

Conclusions

In this paper a methodology to convert a multibody vehicle model into a high-fidelity real-time model was presented. The main conclusions are:

- the methodology here presented to convert the MBM to the RTM, with the nominal vehicle configuration, already allows a good level of conversion accuracy, hence the converted model has proved adequate for both handling and longitudinal dynamics simulations;
- the proposed optimization loop improves the results of the directly converted real-time vehicle model: the root mean square error of each maneuver is drastically reduced, thus remaining within the desired percentage tolerance;
- the adopted assumptions for each subsystem, such as the nonlinear 2D maps for the suspension elasto-kinematics, revealed suitable, as demonstrated in the results section;
- the presented fitness function is properly designed to include the root mean square error from different targets. Although the optimized results are trade-offs between these tasks, the overall vehicle fitting is improved;
- the set of selected tunable parameters significantly changes the vehicle steady state and transient response: their boundary conditions are properly identified to keep them within physical limit values;

- in future development a more detailed steering subsystem could be included also considering the steering line stiffness (torsion bar) and the power steering (EPS or HPS).

References

1. Guiggiani, M., The Science of Vehicle Dynamics 2nd Edition (Springer, 2018).
2. Galvagno, Enrico, et al. Experimental-Numerical Correlation of a Multi-Body Model for Comfort Analysis of a Heavy Truck. No. 2020-01-0768. SAE Technical Paper, 2020, doi: 10.4271/2020-01-0768.
3. Vella, A. D., Lisitano, D., Tota, A., & Wang, B. (2020). Analysis of heavy commercial vehicle cornering behaviour through a multibody model. Int. J. Mech. Control, 21(2), 39-50.
4. Bonisoli, Elvio, Domenico Lisitano, and Luca Dimauro. "Detection of critical mode-shapes in flexible multibody system dynamics: The case study of a racing motorcycle." Mechanical Systems and Signal Processing 180 (2022): 109370.
5. Tumasov, Anton, et al. "Estimation of light commercial vehicles dynamics by results of road tests and simulation." International Design Engineering Technical Conferences and Computers and Information in Engineering Conference. Vol. 46346. American Society of Mechanical Engineers, 2014.
6. Parra, A., Cagigas, D., Zubizarreta, A., Rodríguez, A. J., & Prieto, P. (2019, October). Modelling and validation of full vehicle model based on a novel multibody formulation. In IECON 2019-45th Annual Conference of the IEEE Industrial Electronics Society (Vol. 1, pp. 675-680). IEEE.
7. Kim, S. S., & Jeong, W. (2007). Subsystem synthesis method with approximate function approach for a real-time multibody vehicle model. Multibody System Dynamics, 17(2), 141-156.
8. Galvagno, E., Galfrè, M., Mari, G., Velardocchia, M., & Tota, A. (2021). A Methodology for Parameter Estimation of Nonlinear Single Track Models from Multibody Full Vehicle Simulation (No. 2021-01-0336). SAE Technical Paper, doi: 10.4271/2021-01-0336
9. IPG Automotive GmbH CarMaker add on: "Adams2CM converter".https://ipg-automotive.com/en/products-solutions/software/add-ons/
10. "Adams/Car to CarSim automatic converter": https://www.carsim.com/publications/newsletter/images/AMET_AutoConvA2C_Brochure_2017.pdf
11. Adams/Car to Vi-CarRealTimehttps://www.vi-grade.com/en/products/vi-carrealtime/
12. IPG Automotive GmbH "CarMaker: Virtual testing of automobiles and light-duty vehicles", [online] Available at: https://ipg-automotive.com/en/products-solutions/software/carmaker/
13. Vetturi, D. A. V. I. D., et al. "Genetic algorithm for tyre model identification in automotive dynamics studies." The 29th ISATA2 International Symposium on Automotive Technology and Automation, Florence, Italy. 1996.
14. Ormándi, Tamás, Balázs Varga, and Tamás Tettamanti. "Estimating vehicle suspension characteristics for digital twin creation with genetic algorithm." Periodica Polytechnica Transportation Engineering 49.3 (2021): 231-241.
15. Bonisoli, E., Velardocchia, M., Moos, S., Tornincasa, S., & Galvagno, E. (2010). Gearbox Design by means of Genetic Algorithm and CAD/CAE Methodologies (No. 2010-01-0895). SAE Technical Paper, doi: 10.4271/2010-01-0895
16. Bonisoli, E., A. D. Vella, and S. Venturini. "Uncertainty Effects on Bike Spoke Wheel Modal Behaviour." Model Validation and Uncertainty Quantification, Volume 3. Springer, Cham, 2023. 111-123.
17. Paluskar, P., & Vaidya, R. (2011). Taguchi method (DOE) based performance optimization of a three link rigid axle passenger car suspension using MBD simulations (No. 2011-01-0734). SAE Technical Paper, doi:10.4271/2011-01-0734.
18. Derrix, Daniel, et al. "Experimental Analysis of the Influence of Body Stiffness on Dynamic Suspension Kinematics and Compliance Characteristics and Dynamic Body Behavior." *SAE International Journal of Vehicle Dynamics, Stability, and NVH* 5.10-05-04-0032 (2021): 475-487.
19. Harrer, Manfred, and Peter Pfeffer, eds. Steering handbook. Vol. 163. Cham, Switzerland: Springer International Publishing, 2017.
20. Audet, Charles, and John E. Dennis Jr. "Analysis of generalized pattern searches." SIAM Journal on optimization 13.3 (2002): 889-903.
21. International Organization for Standardization, ISO 7401:2003, "Road Vehicles – Lateral Transient Response Test Methods – Open-loop Test Method," International Organization for Standardization (2003)

Contact Information

luca.zerbato@polito.it

Definitions/Abbreviations

MBM	Multibody model
RTM	Real-Time model
LCV	Light commercial vehicle
EPS	Electric power steering
HPS	Hydraulic power steering
TP	Percentage tolerance
PF	Penalty factor
RMSE	Root mean square error
OEM	Original equipment manufacturer
ADAS	Advanced driver-assistance devices
GA	Genetic algorithm
k&c	Kinematic and compliance